

# Plasmonic biosensors with biocompatible nanosilver

G.A. Sotiriou<sup>\*</sup>, T. Sannomiya<sup>\*\*</sup>, A. Teleki<sup>\*</sup>, J. Voros<sup>\*\*</sup> and S.E. Pratsinis<sup>\*</sup>

<sup>\*</sup>Particle Technology Laboratory, sotiriou@ptl.mavt.ethz.ch

Institute of Process Engineering, Department of Mechanical and Process Engineering

<sup>\*\*</sup>Laboratory of Biosensors and Bioelectronics, Department of Information Technology and Electrical Engineering

Swiss Federal Institute of Technology (ETH Zurich)

Sonneggstrasse 3, CH-9092, Zurich, Switzerland

## ABSTRACT

The plasmonic properties of noble metal nanoparticles facilitate their use in novel in-vivo bio-applications such as targeted drug delivery and cancer cell therapy. Nanosilver is best suited for such applications as it has the lowest plasmonic losses among all such materials in the UV-visible spectrum. Its toxicity, however, can destroy the surrounding healthy tissue and thus, hinders its safe employment. Here, that toxicity against a model biological system (*Escherichia coli*) is “cured” by coating nanosilver hermetically with a thin SiO<sub>2</sub> layer by a scalable flame aerosol method without reducing its plasmonic performance. This creates the opportunity to safely use powerful nanosilver for intracellular bio-applications. The label-free biosensing and surface bio-functionalization of these ready-to-use, non-toxic (benign) nanosilver particles is presented here by measuring the adsorption of bovine serum albumin (BSA) in a model sensing experiment. Furthermore, the silica coating around nanosilver prevents its agglomeration or flocculation and thus, enhances its biosensitivity.

**Keywords:** silver nanoparticles, silicon dioxide, antibacterial activity

## 1 INTRODUCTION

Noble metal (e.g. gold or silver) nanoparticles possess plasmonic properties that are attractive in novel biological sensing applications [1]. These unique optical properties originate from collective oscillations of conduction electrons, the so-called localized surface plasmons [2]. These properties do not degrade over time and depend on nanoparticle shape and size as well as on the refractive index of their surroundings [3]. For label-free biosensing, protein molecules which have a higher refractive index than aqueous solutions cause a red shift of the plasmon absorption band [2]. The latter dependency can be exploited to detect biomolecules such as proteins.

Certain diseases such as bacterial infections or cancer are accompanied by a higher concentration of specific analytes. Such target analytes are known to bind specifically to the corresponding capture biomolecules (e.g.

antibodies) [2]. Thus, by anchoring the latter on the surface of plasmonic biosensors (bio-functionalization), their detection is possible by the local change in the refractive index. In fact, this has been exploited by multi-step synthesis of plasmonic sensors including rods [4] or disks [5] that exhibit promising ultra-sensitive biodetection performance, bringing plasmonic biosensors close to detection limits achieved by other techniques. Moreover, plasmonic nanoparticles strongly scatter and absorb light enabling their detection under dark field illumination [6]. So they have been used as intracellular in-vivo biomarkers and as diagnostic or even therapeutic tools [7] for targeted drug delivery or cancer cell treatment [8].

Among noble metal nanoparticles, nanosilver is ideal as it has the lowest plasmonic losses in the UV-visible spectrum [9]. There is, however, concern regarding toxicity and environmental impact of nanosilver that blocks its use in bio-applications. In fact, nanosilver is the first nanomaterial to draw the attention of the U.S. Environmental Protection Agency (EPA) [10]. Nanosilver is toxic to biological systems by its direct contact with cells and/or release of toxic Ag<sup>+</sup> ions from its surface [11]. If the toxicity of nanosilver would be controlled and essentially “cured”, new opportunities would be created in intracellular biosensing and bio-imaging.

A potent way to achieve this is by applying hermetically a thin, transparent and inert silica-coating around the nanosilver surface. The role of such silica shell is triple a) inhibits the toxicity of nanosilver by preventing the direct contact of cells with its surface, b) blocks the release of toxic Ag<sup>+</sup> ions and c) facilitates the colloidal dispersion of nanosilver particles that otherwise flocculate and exhibit limited biosensitivity [3]. Additionally, it facilitates surface functionalization of nanosilver with bio-molecules since the surface chemistry of silica is reasonably well understood [12]. Such nanosilver-silica core-shell particles have been made already by employing silane coupling agents [12], sol-gel and reverse microemulsion [13]. Such wet-coated nanosilver, however, retains its toxicity, most probably because such SiO<sub>2</sub> shells tend to be porous [14] enabling toxic Ag<sup>+</sup> ion transport, and thus hindering the use of nanosilver as in-vivo biomarker.

Here, encapsulation of nanosilver with silica is made in one-step by a dry, scalable [15] flame aerosol method [16].

The influence of this coating on nanosilver toxicity is investigated here against a model biological system, the Gram-negative bacterium *Escherichia coli* (*E. coli*). The effect of SiO<sub>2</sub> coating on the plasmonic properties of nanosilver is measured and finally, the feasibility of these core-shell particles as biosensors is demonstrated in the presence of adsorbed bovine serum albumin (BSA) which serves as a model protein [17].

## 2 EXPERIMENTAL

Nanosilver particle production and *in-situ* SiO<sub>2</sub> coating was achieved in a modified flame aerosol reactor which is described in detail elsewhere [16]. In brief, a precursor solution containing 0.5 M Ag-benzoate (Sigma Aldrich, purity 99%) dissolved in 2-ethylhexanoic acid (Sigma Aldrich, purity ≥99%) and benzonitrile (Sigma Aldrich, purity ≥99%) (volume ratio 1:1) was fed through a capillary (feed rate 5 mL/min) and dispersed by oxygen (PanGas, purity >99.9%, flow rate: 5 L/min) and combusted forming the Ag nanoparticles. The freshly-formed core Ag nanoparticles were coated in-flight by swirl injection of hexamethyldisiloxane (HMDSO, Sigma Aldrich, purity ≥99%) vapor along with 15 L/min nitrogen (PanGas, purity >99.9%) at room temperature through a metallic ring with 16 equidistant openings. The ring was placed on top of a 20-30 cm long quartz glass tube. The reactor was terminated by a 25 cm quartz glass tube. The HMDSO vapor was supplied by bubbling nitrogen through approximately 350 mL liquid HMDSO in a 500 mL glass flask. The SiO<sub>2</sub> content in the product particles was calculated at full saturation [16] and by varying the bubbler temperature (5-7 °C) and nitrogen flow rate (0.05-0.3 L/min). The N<sub>2</sub> stream carrying HMDSO vapor to the coating ring outlet is fully saturated with HMDSO up to 0.8 L/min N<sub>2</sub> flow rate through the HMDSO bubbler [16]. The full conversion of HMDSO to SiO<sub>2</sub> has been proven by DC plasma optical emission spectroscopy for SiO<sub>2</sub>-coated TiO<sub>2</sub> nanoparticles [16], produced with the same enclosed flame aerosol reactor.

High resolution transmission electron microscopy (HRTEM) was performed with a CM30ST microscope or a Tecnai F30 microscope (both: FEI; LaB6 cathode, operated at 300 kV, point resolution ~2 Å). Product particles were dispersed in ethanol and deposited onto a perforated carbon foil supported on a copper grid.

A growth inhibition assay was performed to examine the toxicity of the nanosilver particles. Therefore, *E. coli* JM101 bacteria synthesizing green fluorescent protein (GFP) from a plasmid-encoded gene were grown in Luria-Bertani broth (LB) [18] at 37 °C overnight. The culture was subsequently diluted with LB by mixing 25 µL of the culture in 5 ml LB. The nanosilver particle concentration was normalized with respect to their surface area. All measurements have an equal Ag surface concentration of approximately  $2.3 \cdot 10^{-4}$  m<sup>2</sup>/mL. The nanosilver particles were dispersed in de-ionized water by ultrasonication

(Sonics vibra-cell) for 20 seconds at 75% amplitude, with a pulse configuration on/off of 0.5s/0.5s. For the assay, 50 µL of the aqueous solutions containing the dispersed nanosilver particles were added to 50 µL of the diluted cells. The growth of *E. coli* JM101 was investigated by monitoring the fluorescent signal of the GFP (Perkin Elmer 1420) corrected for background fluorescence. The growth percentages were calculated by assuming 100% growth for the control measurements (no silver). The error bars for each data point were obtained as the standard deviation of 4 measurements.

The biosensing of nanosilver particles was assessed using bovine serum albumin (BSA) as model protein. Oxygen-plasma-cleaned (Harrick Plasma PDC32G, 18W, 2min) glass slides were coated by poly(L-lysine), PLL, by incubating the substrate surface with PLL solution (100 mg/L). Nanosilver particles were then deposited from the aqueous suspension onto the PLL-coated glass substrate. The positively charged PLL layer immobilizes the negatively charged nanoparticles by electrostatic force (both silver and silica are negatively charged at pH 7). The substrate was then set in a flow cell which was mounted on a UV/vis spectrometer (Cary Varian 500) and the Ag plasmon absorption peak positions were monitored during BSA adsorption. The measurement was started in a buffer solution consisting of 10 mM 4-(2-hydroxyethyl) piperazine-1-ethanesulfonic acid (HEPES) with a pH adjusted to 7.4 using NaOH and supplemented with 150 mM NaCl. The BSA solution (100 mg/L in HEPES) was then injected followed by rinsing with HEPES buffer solution to confirm the adsorption signal. The peak position was determined by parabolic fitting of the absorption bands.

## 3 RESULTS AND DISCUSSION

### 3.1 SiO<sub>2</sub> coating “cures” nanosilver toxicity

Figure 1 shows TEM images of the 1.4 (a) and 7.8 wt% (b) SiO<sub>2</sub>-coated nanosilver. The surface of the low SiO<sub>2</sub>-content nanosilver particles (Fig. 1a) is bare or coated with a very thin, non-continuous, amorphous, “patchy” SiO<sub>2</sub> layer (< 1 nm) [16]. TEM image of the 7.8 wt% SiO<sub>2</sub> sample (Fig. 1b) shows that a thin amorphous SiO<sub>2</sub> layer surrounds the crystal core nanosilver particles. The amorphous SiO<sub>2</sub> shell is approximately 2-5 nm thick. Furthermore, a close observation of high silica-content nanosilver particles shows that these particles are partially aggregated as the silica coating bridges 5-6 particles there (Fig. 1b).

Figure 2 shows the *E. coli* population after 390 minutes at 37 °C (represented as *E. coli* fluorescence) as a function of the SiO<sub>2</sub> content. The population after 390 minutes in the absence of nanosilver (no particles or only SiO<sub>2</sub>) is also shown (star, broken line). For the low SiO<sub>2</sub> content (1.4 wt%) nanosilver, the *E. coli* growth is almost half of the control. These samples are partially coated, as illustrated in the transmission-electron-microscope (TEM) image of the

1.4 wt% SiO<sub>2</sub> sample, and thus their Ag surface is partially exposed, contributing to the reduction of the *E. coli* population. For the higher SiO<sub>2</sub> contents (7.8 and 9.5 wt%), however, the *E. coli* growth is hardly inhibited, within experimental error. The TEM image of the 7.8 wt% SiO<sub>2</sub> sample (Fig. 1b) shows that a thin SiO<sub>2</sub> layer surrounds the core nanosilver particles, which largely prevents the toxic action of the latter and thus may have “cured” their toxicity.

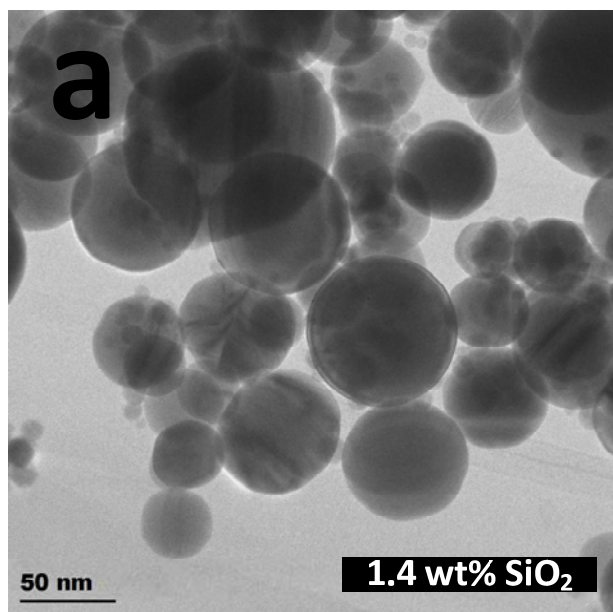


Figure 1. TEM images of the 1.4 wt% (a) and 7.8 wt% (b) SiO<sub>2</sub> coated nanosilver. Patchy coatings of nanosilver with bare surface as well as with very thin (<1 nm), non-continuous amorphous SiO<sub>2</sub>-coating are observable. The nanosilver core can be distinguished from its amorphous silica coating. Adopted from [17].

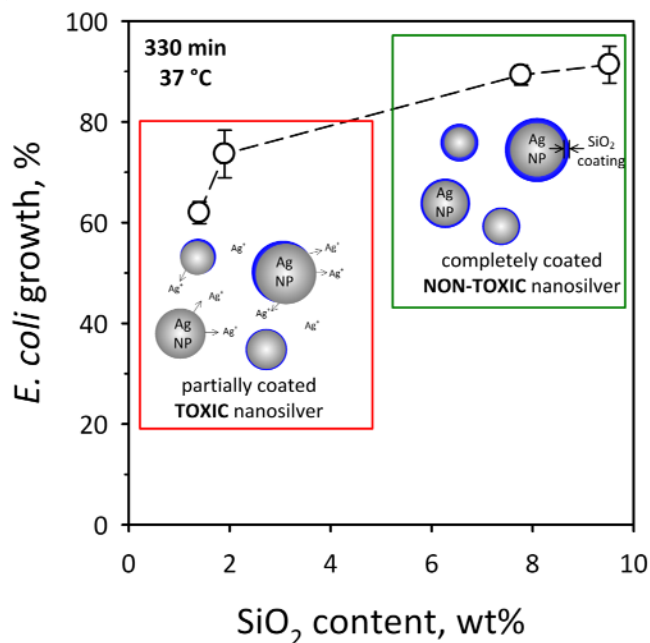


Figure 2. The *E. coli* growth (100% corresponds to the growth of only *E. coli*) is shown as a function of SiO<sub>2</sub> content. Adopted from [17].

### 3.2 Biosensing performance

Figure 3 presents the biosensing performance of the fully coated nanosilver (SiO<sub>2</sub> contents 9.5 wt%). The sensor response  $\Delta\lambda$  (shift of the peak position) is expressed as a function of time for the SiO<sub>2</sub>-coated nanosilver. As soon as the sensor response stabilizes with the buffer solution ( $t = 0$  min), BSA is added. When the adsorption of BSA reaches a stable signal at about  $t = 25$  min, the buffer solution is injected again for rinsing to exclude the effect of the medium change. It can be observed that the adsorption of BSA follows the expected saturation curve. The non-toxic fully-coated biosensors reach a sensor response of  $\sim 3$  nm. This could be attributed to their reduced effective surface area of partially-coated nanosilver by flocculation. Therefore, the SiO<sub>2</sub> coating, apart from reducing nanosilver toxicity, also can be used as biosensors.

## 4 CONCLUSIONS

The toxicity of nanosilver can be drastically reduced by a thin hermetic coating on its surface. This results in a safe biomaterial ready to be employed as diagnostic and/or therapeutic agent without inducing any damage to the surrounding healthy tissue. The hermetic SiO<sub>2</sub> layer prevents the direct contact of cells with the nanosilver surface and blocks the toxic Ag<sup>+</sup> ion release. This was demonstrated here by the one-step synthesis of *in-situ* SiO<sub>2</sub>-coated nanosilver particles by a scalable flame technology resulting in core-shell nanostructures. The feasibility of silica-coated nanosilver as biosensor was shown by monitoring its plasmon absorption band in the presence of

physically adsorbed BSA on the nanosilver surface. The prevention of the nanosilver agglomeration enhanced the biosensor performance, as fully-coated nanosilver outperformed the partially-coated. The fast, one-step silica encapsulation of nanosilver resulted in non-toxic plasmonic biosensors with promising performance.

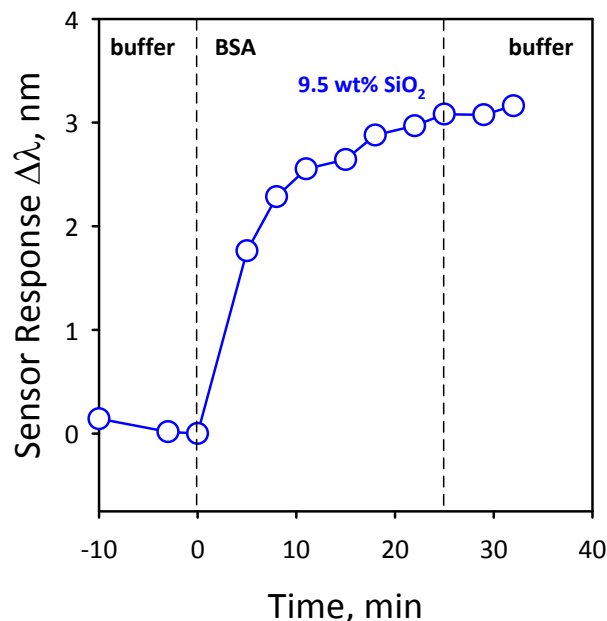


Figure 3. The sensor response  $\Delta\lambda$  as a function of time for the fully-coated ( $\text{SiO}_2$  content 9.5 wt%) nanosilver.

## REFERENCES

- [1] Alivisatos, P. The use of nanocrystals in biological detection. *Nature Biotechnology* **22**, 47-52 (2004).
- [2] Willets, K. A. & Van Duyne, R. P. Localized surface plasmon resonance spectroscopy and sensing. *Annu. Rev. Phys. Chem.* **58**, 267-297 (2007).
- [3] Evanoff, D. D. & Chumanov, G. Synthesis and optical properties of silver nanoparticles and arrays. *ChemPhysChem* **6**, 1221-1231 (2005).
- [4] Kabashin, A. V., Evans, P., Pastkovsky, S., Hendren, W., Wurtz, G. A., Atkinson, R., Pollard, R., Podolskiy, V. A. & Zayats, A. V. Plasmonic nanorod metamaterials for biosensing. *Nature Mater.* **8**, 867-871 (2009).
- [5] Chen, S., Svedendahl, M., Kall, M., Gunnarsson, L. & Dmitriev, A. Ultrahigh sensitivity made simple: nanoplasmonic label-free biosensing with an extremely low limit-of-detection for bacterial and cancer diagnostics. *Nanotechnology* **20**, 434015-434024 (2009).
- [6] Wax, A. & Sokolov, K. Molecular imaging and darkfield microspectroscopy of live cells using gold plasmonic nanoparticles. *Laser & Photonics Reviews* **3**, 146-158 (2009).
- [7] Jain, P. K., Huang, X., El-Sayed, I. H. & El-Sayad, M. A. Review of some interesting surface plasmon resonance-enhanced properties of noble metal nanoparticles and their applications to biosystems. *Plasmonics* **2**, 107-118 (2007).
- [8] Loo, C., Lowery, A., Halas, N., West, J. & Drezek, R. Immunotargeted nanoshells for integrated cancer imaging and therapy. *Nano Lett.* **5**, 709-711 (2005).
- [9] Barnes, W. L., Dereux, A. & Ebbesen, T. W. Surface plasmon subwavelength optics. *Nature* **424**, 824-830 (2003).
- [10] Erickson, B. E. Nanosilver pesticides. *Chem. Eng. News* **87** (48), 25-26 (2009).
- [11] Sotiriou, G. A. & Pratsinis, S. E. Antibacterial activity of nanosilver ions and particles. *Environmental Science & Technology* **44**, 5649-5654 (2010).
- [12] Liz-Marzan, L. M., Giersig, M. & Mulvaney, P. Synthesis of nanosized gold-silica core-shell particles. *Langmuir* **12**, 4329-4335 (1996).
- [13] Han, Y., Jiang, J., Lee, S. S. & Ying, J. Y. Reverse microemulsion-mediated synthesis of silica-coated gold and silver nanoparticles. *Langmuir* **24**, 5842-5848 (2008).
- [14] Xu, K., Wang, J. X., Kang, X. L. & Chen, J. F. Fabrication of antibacterial monodispersed Ag-SiO<sub>2</sub> core-shell nanoparticles with high concentration. *Materials Letters* **63**, 31-33 (2009).
- [15] Mueller, R., Madler, L. & Pratsinis, S. E. Nanoparticle synthesis at high production rates by flame spray pyrolysis. *Chem. Eng. Sci.* **58**, 1969-1976 (2003).
- [16] Teleki, A., Heine, M. C., Krumeich, F., Akhtar, M. K. & Pratsinis, S. E. In situ coating of flame-made TiO<sub>2</sub> particles with nanothin SiO<sub>2</sub> films. *Langmuir* **24**, 12553-12558 (2008).
- [17] Sotiriou, G. A., Sannomiya, T., Teleki, A., Krumeich, F., Vörös, J. & Pratsinis, S. E. Non-Toxic Dry-Coated Nanosilver for Plasmonic Biosensors. *Adv. Funct. Mater.* **20**, 4250-4257 (2010).
- [18] Sambrook, J. & Russell, D. W. *Molecular Cloning: A Laboratory Manual*. 3 edn, (NY Cold Spring Harbor Laboratory Press, 2001).